

On the Structure and Vibrational Spectrum of Tetrabromothiophene

Frank Blockhuys, Bart Rousseau, Luc D. Peeters, Christiaan Van Alsenoy, and Herman J. Geise*

University of Antwerpen (UIA), Department of Chemistry, Universiteitsplein 1, B-2610 Antwerpen (Wilrijk) Belgium

Olga N. Kataeva

A. E. Arbutov Institute of Organic and Physical Chemistry, Russian Academy of Sciences, A.E. Arbutov str. 8, Kazan 420088, Russia

Benjamin Van der Veken and Wouter A. Herrebout

University of Antwerpen (RUCA), Department of Inorganic Chemistry, Groenenborgerlaan 171, B-2020 Antwerpen, Belgium

Received: March 31, 2000; In Final Form: July 31, 2000

The gas phase structure and vibrational spectrum of tetrabromothiophene are calculated by ab initio methods. Unscaled DFT/B3LYP/TZVP frequencies fit conveniently well to the solid phase Raman spectrum and helped to establish the crystal space group. The unusual fit and the compounds' solidification into very small, irregularly arranged crystallites are correlated to the screening of the thiophene moiety by the bromine atoms.

Introduction

Tetrabromothiophene (henceforth abbreviated TBT) is one of the few examples of an organic molecule in which the usual outside lining of small, hard hydrogen atoms is replaced by one of large, soft, electron rich bromine atoms. The possible consequences on the properties of the thus screened thiophene π -system has attracted much attention. The list of material characteristics already investigated includes dipole moment,^{1,2} linear dichroism,³ thermodynamic functions,⁴ and ¹³C nuclear magnetic resonance,⁵ and ⁷⁹Br nuclear quadrupole resonance,⁶ UV/vis,⁷ IR/Raman spectroscopic,^{4,8} and mass spectrometric^{9,10} data. Strikingly lacking from this list, however, is the *geometry* of tetrabromothiophene. Shimozawa² made some structural assessments when trying to explain the large difference between the observed and calculated dipole moments, but these were limited by his experimental measurements—he himself suggested that a more thorough analysis of the compound's structure should be made in order to make a better assessment of the mentioned difference.

To fill the gap, we set out to study the structure theoretically by ab initio methods and experimentally by diffraction techniques. Gas electron diffraction as well as solid-state X-ray diffraction come into consideration. The former because TBT can be sublimated, the latter because TBT is the only brominated thiophene derivative with a high melting point. Although all efforts to produce suitable single crystals failed so far, the crystal structure has recently been determined¹¹ using powder diffraction methods; the gas phase geometry will be reported on later. Here, we report on the ab initio calculated geometry of tetrabromothiophene using both Hartree–Fock and density functional methods and on the vibrational spectra obtained. Much attention is given to the interplay between solid-state packing and

vibrational spectroscopic behavior. Figure 1 shows the molecular structure and the numbering of the atoms.

Experimental Section

Tetrabromothiophene was synthesized via direct bromination of thiophene using an excess of bromine, according to Paal.¹² The compound was purified by copious washings with methanol and isolated with an overall yield of 97%. The white powder (mp 118–121 °C; lit. 117–118 °C¹³) was analyzed with GC and proved to be pure. ¹H NMR (acetone-*d*₆): no signals. ¹³C NMR (acetone-*d*₆): $\delta = 111.5$ ppm (s, C₂ and C₅), $\delta = 117.6$ ppm (s, C₃ and C₄) (lit.: in CS₂, $\delta = 112.0$ and $\delta = 118.8$ ppm, respectively⁵). All δ values are relative to tetramethylsilane. Attempts were made to grow single crystals by recrystallization from various solvents and by sublimation, but no crystals suitable for single-crystal X-ray diffraction were obtained.

IR spectra of solid tetrabromothiophene were recorded between 4000 and 400 cm⁻¹ on a Bruker 66v interferometer, using a global source, a Ge/KBr beam splitter and a deuterated triglycine sulfate detector (DTGS), at a resolution of 2 cm⁻¹. The Raman spectra were recorded from the powder held in a Pyrex capillary, using a Spex 1403 double monochromator and 200 mW of the 514 nm radiation of an Ar-ion laser. The spectrometer was fitted with the Spex premonochromator to filter out unwanted plasma lines. For survey spectra a resolution of 4 cm⁻¹ was used, while the more intense bands and the low-frequency region were also investigated at 1 cm⁻¹ resolution.

Computational Methods

All HF calculations were performed using Pulay's gradient method^{14,15} incorporated in the program BRABO for large molecules.^{16,17} The geometries for different combinations of basis sets were calculated with complete relaxation until convergence was reached; for convergence criteria see ref 18.

* To whom correspondence should be addressed. Fax: +32-3-820-23-10. E-mail: latifa@uia.ua.ac.be.

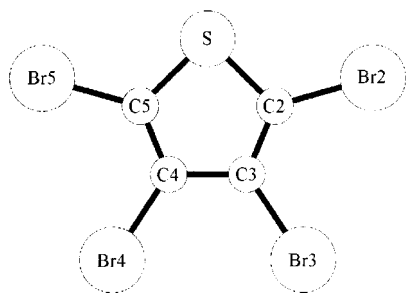


Figure 1. Molecular structure and atomic numbering of tetrabromothiophene.

The geometrical results are given in Table 1: geometry I was calculated using 3-21G on carbon¹⁹ and 33-21G* on sulfur^{20,21} and bromine,²² II using 6-31G* on carbon²³ and 33-21G* on sulfur and bromine, III using 6-31G* on both carbon and sulfur^{20,24} and 6-311G* on bromine,²⁵ and IV using the ahl-svp basis set²⁶ on all three elements. Beginning from a nonplanar starting geometry, all calculations led to a planar final model having C_{2v} symmetry. Equally, the compound's geometry was calculated at the DFT-B3LYP/Ahrlrichs TZVP^{26–28} level of theory, assuming C_{2v} symmetry. These results obtained using Gaussian 94,²⁹ are given in Table 1, as set V.

The approach of increasing sophistication of basis sets and methods was taken since at the beginning we were unable to match the theoretical IR frequencies with the experimental ones given in ref 4.

Starting from the optimized geometries I and II, we calculated the corresponding force fields and frequencies and tried to fit them to the experimentally determined values. The best we could obtain was a largest difference of 77 cm^{-1} and a rms deviation of 31 cm^{-1} for I, and a largest difference of 106 cm^{-1} and a rms deviation of 36 cm^{-1} for II. In both cases we used two scaling-factors: 0.82 for all stretching modes and 0.74 for all remaining modes. At this point we decided to remeasure the vibrational spectra and to use the most sophisticated theoretical model.

Frequencies, based on the unscaled force field of structure V, calculated on the DFT/B3LYP/TZVP level, and using the Gaussian 94 program package,²⁹ compared very favorable with our newly recorded Raman spectra. Table 2 lists the unscaled frequencies and shows a root-mean-square deviation of 17 cm^{-1} and a largest difference of 39 cm^{-1} between calculated and experimental values.

Vibrational Spectra

The Raman spectrum of tetrabromothiophene was reported for the first time by Kohlrausch et al.⁸ More recently, the IR spectrum of the compound in solution and in the solid state and the Raman spectrum of the solid state have been discussed by Faniran.⁴ The agreement between the literature data and our theoretical results, as was mentioned above, was far from satisfactory, and some of the assignments in the literature⁴ must be doubted. This is most clearly seen in the low frequency region: Faniran has assigned only 4 of the 21 fundamentals to frequencies below 250 cm^{-1} , the other bands observed in this region being assigned as lattice modes. However, our calculations suggest, in agreement with the high molecular mass of the molecule, that in this region no less than 9 internal modes must be expected. Moreover, as will be discussed below, the recent X-ray study of the compound has shown that the unit cell contains 4 molecules, which should give rise to splittings of the fundamental modes in the solid-state spectra, none of

which have been discussed by Faniran. In view of this it was judged useful to reinvestigate the solid-state spectra.

The published IR spectrum of the solid⁴ is clearly influenced by the Christiansen effect. This is a distortion of the absorption bands due to superposition of absorption and reflectance spectra. The effect arises when the crystallites in the sample are of similar size as the radiation wavelengths and occurs especially with plate-shaped crystallites. The samples used in this study caused similar problems. Repeated crystallization from CCl_4 did not improve the spectra, and similar results were obtained by running spectra from samples deposited on a KBr window by evaporating a CCl_4 solution. Therefore, our IR spectra are essentially similar to those of Faniran.

The Raman spectra recorded in this study, however, are at variance with the one in the literature⁴ in two ways. First, six bands prominently visible in the published spectrum are absent from our spectra, and our intensity pattern between 125 and 100 cm^{-1} is remarkably different from the one observed before.⁴ Second, due to a superior signal-to-noise ratio in our spectra, a number of weak bands have been observed that were unnoticed before.

The published liquid and solid-state IR spectra⁴ (disregarding Christiansen distortion) are rather similar, which shows that the splittings in the factor group multiplets in general are small. This is in line with the expectations for a molecular crystal. However, for a limited number of modes in the Raman spectra factor group splittings have been observed. This is illustrated in Figure 2, which gives the Raman spectrum of the solid between 1430 and 1370 cm^{-1} . Inspection of the ab initio calculations shows that only one fundamental of the isolated molecule must be expected in this region, while it can be seen that the 1406 cm^{-1} band is split in at least 3 components. This observation is of importance to identify the space group of TBT in the solid (see below). To make that identification, we need to establish the existence (if any) of mutual exclusion of IR and Raman modes and to diagnose the occurrence of factor group splittings. With only good quality, solid-state Raman spectra available, and lacking additional single-crystal data, the Raman frequencies must be assigned with great care. To do so, we will start ignoring the splittings in the following paragraphs and first discuss the observed bands in terms of the modes of the isolated molecule (C_{2v} symmetry). The latter will be identified by their Herzberg system number (see Table 2).

Only three fundamentals are predicted above 1100 cm^{-1} . The assignment of the intense Raman band at 1406.1 cm^{-1} to $\nu_1(a_1)$, predicted at 1439 cm^{-1} , and the equally intense band at 1271 cm^{-1} to $\nu_2(a_1)$, predicted at 1259 cm^{-1} , is straightforward, while the assignment of the much weaker band at 1484 cm^{-1} to $\nu_{15}(b_2)$ is supported by the observation of a very intense IR band at 1491 cm^{-1} .

With the exception of $\nu_{17}(b_2)$, the modes predicted in the $900\text{--}300\text{ cm}^{-1}$ region, i.e., $\nu_3\text{--}\nu_5$, ν_9 , ν_{12} , $\nu_{16}\text{--}\nu_{19}$, have frequencies sufficiently close to observed Raman bands to allow an unique assignment. Near 836 cm^{-1} , the frequency where $\nu_{17}(b_2)$ is predicted, an extremely weak feature, hardly recognizable above the noise, is detected in the Raman spectrum near 865 cm^{-1} . In the IR spectrum, however, a strong band is found at 864 cm^{-1} , so that the assignment of ν_{17} to this band is clear.

Between 1050 and 900 cm^{-1} only two modes, $\nu_{16}(b_2)$ and $\nu_3(a_1)$, are predicted, at 998 and 957 cm^{-1} , while bands at 1008 , 982.5 , and 967 cm^{-1} are found in the Raman spectrum. In view of the above considerations, we assign the lower two bands as a factor group doublet due to $\nu_3(a_1)$, and the band at 1008 cm^{-1}

TABLE 1: Calculated Gas Phase Geometrical Results (Columns I–V) and X-ray Powder Diffraction Results with Least-Squares Obtained esd's in Parentheses¹¹ in the Last Column

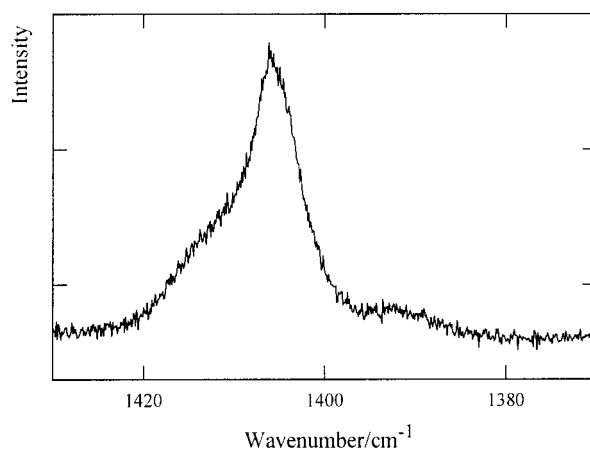
	I	II	III	IV	V	\Delta	exp
S–C(2)	1.724	1.719	1.727	1.726	1.747	0.048	1.699(5)
C(2)–C(3)	1.345	1.341	1.344	1.349	1.362	0.036	1.398(8)
C(3)–C(4)	1.444	1.440	1.448	1.449	1.438	0.007	1.431(4)
C(4)–C(5)	1.345	1.341	1.344	1.349	1.362	0.039	1.401(9)
C(5)–S	1.724	1.719	1.727	1.726	1.747	0.047	1.700(5)
C(2)–Br(2)	1.868	1.855	1.869	1.862	1.879	0.073	1.952(3)
C(3)–Br(3)	1.870	1.859	1.874	1.868	1.888	0.065	1.953(6)
C(4)–Br(4)	1.870	1.859	1.874	1.868	1.888	0.048	1.936(6)
C(5)–Br(5)	1.868	1.855	1.869	1.862	1.879	0.083	1.962(4)
S–C(2)–C(3)	112.55	112.41	112.59	112.38	112.07	1.0	113.1(3)
C(2)–C(3)–C(4)	112.07	112.13	112.06	112.08	112.60	3.4	109.2(5)
C(3)–C(4)–C(5)	112.07	112.13	112.06	112.08	112.60	4.2	108.4(5)
C(4)–C(5)–S	112.55	112.41	112.59	112.38	112.07	0.7	112.8(3)
C(5)–S–C(2)	90.77	90.92	90.70	91.08	90.68	4.1	86.6(2)
S–C(2)–Br(2)	120.21	120.23	119.24	119.41	119.55	7.7	111.9(3)
C(2)–C(3)–Br(3)	124.61	124.54	124.51	124.40	123.86	5.2	129.1(3)
C(3)–C(4)–Br(4)	123.32	123.33	123.42	123.52	123.54	1.8	121.7(4)
C(4)–C(5)–Br(5)	127.25	127.36	128.17	128.22	128.39	1.5	126.9(4)
S–C(5)–Br(5)	120.21	120.23	119.24	119.41	119.55	5.4	114.2(3)
C(5)–C(4)–Br(4)	124.61	124.54	124.51	124.40	123.86	5.6	129.5(3)
C(4)–C(3)–Br(3)	123.32	123.33	123.42	123.52	123.54	1.7	121.8(4)
C(3)–C(2)–Br(2)	127.25	127.36	128.17	128.22	128.39	2.3	126.1(4)

^a Differences between experimental and calculated (model V) results are given as $|\Delta|$. See Figure 1 for atomic numbering. Bond lengths in ångströms and valence angles in degrees; for explanation of models I through V see text.

TABLE 2: Calculated Vibrational Frequencies (ν_{calc}) of Free TBT Compared to Experimental Solid Phase Raman Frequencies (ν_{exp}), Together with Experimental Relative Intensities (I_{rel}), Assignment of Bands, and Differences Δ ($=\nu_{\text{exp}} - \nu_{\text{calc}}$)

ν_{calc} (cm ⁻¹)	ν_{exp} (cm ⁻¹)	I_{rel}	assignment	Δ (cm ⁻¹)
1523	1484	vw	$\nu_{15}(\text{b}_2)$	39
1439	1413	sh	$\nu_1(\text{a}_1)$	-33
	1406.1	m		
	1393	w,sh		
1259	1271	m	$\nu_2(\text{a}_1)$	12
	1208	vw		
998	1008	w	$\nu_{16}(\text{b}_2)$	10
957	982	w	$\nu_3(\text{a}_1)$	25
	967	vw		
836	865	vw	$\nu_{17}(\text{b}_2)$	29
730	738	w	$\nu_4(\text{a}_1)$	8
	733.5	sh		
616	604	vw	$\nu_9(\text{a}_2)$	-12
553	523	vw	$\nu_{18}(\text{b}_2)$	-30
495	483	vw	$\nu_{12}(\text{b}_1)$	-12
364	373.3	s	$\nu_5(\text{a}_1)$	9
340	339	vw	$\nu_{19}(\text{b}_2)$	-1
250	259	vw	$\nu_{10}(\text{a}_2)$	9
228	232.5	s	$\nu_6(\text{a}_1)$	5
227	230.5	s	$\nu_{20}(\text{b}_2)$	4
211	~220	sh,w	$\nu_{13}(\text{b}_1)$	9
121	123	vw	$\nu_7(\text{a}_1)$	2
113	117.0	m	$\nu_{21}(\text{b}_2)$	4
110	110	s	$\nu_8(\text{a}_1)$	0
84	97	w	$\nu_{14}(\text{b}_1)$	13
48	43	sh	$\nu_{11}(\text{a}_2)$	-8
	40.1	vs		
	38			
	28.6	s	lattice modes	
	21	m		
	17.7	vs		
	13	vs, sh		
	11.5	vs		

to $\nu_{16}(\text{b}_2)$. The factor group splitting of ν_3 , 15.5 cm⁻¹, is considerable, but is of the same order as the splitting of 13 cm⁻¹ between the lower and middle components of the 1406.1 cm⁻¹ triplet in Figure 2. Similarly, in the region of $\nu_4(\text{a}_1)$ two bands are observed, at 738 and 733.5 cm⁻¹, which are assigned as a factor group doublet of ν_4 .

**Figure 2.** Raman spectrum of tetrabromothiophene in a selected region (see text).

Somewhat less clear are the assignments between 300 and 150 cm⁻¹. In this region four modes are predicted: $\nu_{10}(\text{a}_2)$ at 249 cm⁻¹, $\nu_6(\text{a}_1)$ and $\nu_{20}(\text{b}_2)$ at 227 cm⁻¹, and $\nu_{13}(\text{b}_1)$ at 211 cm⁻¹. Experimentally, a weak band at 259.6 and a strongly overlapping doublet, with components at 232.5 and, approximately, 230 cm⁻¹, are observed in the Raman spectrum. The low-frequency slope of the doublet shows some tailing, suggesting that a weak broad band is present near 225 cm⁻¹. It is clear that the 259.3 cm⁻¹ band must be assigned to $\nu_{10}(\text{a}_2)$, but it is not immediately obvious whether the multiplet structure of the 232.5 cm⁻¹ band is due to factor group splitting of a single mode, in which case the other two fundamentals must be very weak and hidden by the observed multiplet, or whether it is due to the presence of three separate fundamentals. With reference to the ab initio calculations, we prefer the second interpretation, in which we assign the observed components in the calculated order.

The four bands observed between 125 and 90 cm⁻¹ are assigned, in the calculated order, to $\nu_7(\text{a}_1)$, $\nu_{21}(\text{b}_2)$, $\nu_8(\text{a}_1)$, and $\nu_{14}(\text{b}_1)$, which are predicted in this vicinity, and the triplet with components at 43, 40.1, and 38 cm⁻¹ is assigned as a factor group multiplet due to $\nu_{11}(\text{a}_2)$, which is predicted at 48 cm⁻¹.

Finally, the bands at 28.6, 21, 17.7, 13, and 11.5 cm^{-1} are assigned as external modes. The data available do not allow to assign these bands in more detail.

Vibrational Behavior and Space Group Symmetry

The normal coordinates of tetrabromothiophene in the C_{2v} point group span the representation $8a_1 + 3a_2 + 3b_1 + 7b_2$. The molecule crystallizes in the orthorhombic system with $Pbcm$ ($\equiv D_{2h}^{11}$) and $Pca2_1$ ($\equiv C_{2v}^5$), given as possible space groups by X-ray powder diffraction.¹¹ The molecule occupies a 4-fold degenerate general position with site symmetry C_s in the former or one with site symmetry C_1 in the latter space group. The 108 degrees of freedom (in either space group) can be subdivided in 24 external modes of which 3 are acoustic, 9 are translational, and 12 are librational modes, the 84 remaining ones are the internal modes. These 84 modes can be subdivided if the factor group is C_{2v} in $21a_1 + 21a_2 + 21b_1 + 21b_2$, or if the factor group is D_{2h} in $14a_g + 14b_{1g} + 14b_{2u} + 14b_{3u} + 7a_u + 7b_{2g} + 7b_{3g} + 7b_{1u}$. This difference in subdivision leads to the following difference in possible crystal splittings.

Each vibrational mode of tetrabromothiophene in a crystal site of C_1 symmetry has symmetry a , and in the corresponding factor group (C_{2v}^5) generates 4 internal modes of symmetry $a_1 + a_2 + b_1 + b_2$. Thus, in the solid phase each molecular mode gives rise to a triplet in the IR and to a quadruplet in the Raman spectrum. On the other hand a vibrational mode of tetrabromothiophene in a crystal site of C_s symmetry has either symmetry a' or a'' . These generate in the corresponding factor group (D_{2h}^{11}) different internal modes: a' generates $a_g + b_{1g} + b_{2u} + b_{3u}$, which would give rise to doublets in IR and Raman spectra. In contrast a'' generates $a_u + b_{1u} + b_{2g} + b_{3g}$ which would give rise to doublets in the Raman, but no splitting in the IR spectrum.

The assignment of the experimental Raman lines has shown (see above) that the number of components was always two or more for all fundamentals for which factor group splittings have been observed. Moreover, IR and Raman active modes would mutually exclude one another, the inversion center present in D_{2h} making all IR active modes *ungerade*, and all Raman active ones *gerade*. Hence, the observation of band splitting in more than two components, and the lack of mutual exclusion between IR and Raman spectra is in accordance with $Pca2_1$ and not with $Pbcm$ as the space group for crystalline tetrabromothiophene.

Considerations on Tetrabromothiophene's Geometry and Crystal Structure

Since vibrational frequencies and geometry are closely related, one might expect that when frequencies match, the geometries of the crystal and gas phase also match to a large extent. However, the differences between the experimental geometry¹¹ and the theoretical one (set V), given in Table 1, significantly exceed the experimental least-squares esd's and are much larger than those usually observed when two different phases are compared. Here, differences in bond lengths reach 0.083 Å for a C–Br bond, and those in valence angles go as high as 7.7°. This may lead one to judge that either the solid phase diffraction experiment is flawed or the calculations are. One of the main conclusions in ref 11 is that the bromine atoms dominate the diffraction diagram, so that C and S positions can be determined only with a relatively low accuracy. Hence, the experimental esd's are most likely underestimated, and no better agreement can be expected, so that the need for an experimental gas phase electron diffraction geometry remains.

The major result of the powder X-ray determination¹¹ is that it allows us to take a closer look at the packing of TBT in the crystal and so to rationalize why it behaves so uncharacteristically for a molecule with an electron rich π -system. Such behavior shows in the somewhat remarkable macroscopic solid-state properties, such as low solubility in a variety of solvents including polar ones and the fact that it solidifies to crystals with a large mosaic spread (over 20°) consisting of crystallites of size similar to the wavelength of IR radiation (5–20 μm), which causes the Christiansen effect as well as the failure to produce suitable X-ray single crystals. Finally, the dimensions of the unit cell with one short and two long axes (see below) suggest an increased chance on platelike crystals and so an enhanced chance on the Christiansen effect. These properties and the surprisingly good match between the experimental *solid* phase and the theoretical “*gas*” phase vibrational frequencies all suggest that the molecule has only weak interactions with its environment. Stated alternatively, TBT seems to be quasi-unaffected by the environment in which it resides.

This can be seen from Figure 3, which shows three drawings of a part of the crystal containing 27 molecules with the atoms represented by spheres with the van der Waals radius of the corresponding element. The tetrabromothiophene crystal can be seen as consisting of tightly packed bromine atoms with here and there sulfur and carbon atoms, interspersed between the bromines. It looks as if the repetition in the crystal (expressed in, e.g., the cell dimensions $a = 12.672$ Å, $b = 4.043$ Å and $c = 16.375$ Å; the van der Waals radius of Br is 1.95 Å) is due only to the bromine atoms and that the carbon and sulfur atoms position themselves in such a way that they fill in the gaps between the bromines. In fact, every Br atom is surrounded quasi-isotropically by seven other Br atoms at distances of 3.75–4.18 Å. We conclude that the pattern in which the Br atoms are arranged is primarily controlled by their strive after a close packing, mediated, but by no means dictated, by the geometry of the thiophene ring. Or stated more precisely, one may build the TBT packing starting from a hexagonal close packing of Br in which per 24 Br atoms 8 are removed to make way for 4 thiophene rings. This process can be executed in more than one way and is indicated by the fact that more than one solution to the powder diffraction pattern was offered. No matter how the ring was positioned, the Br atoms always remained stacked in the same pattern.¹¹

It is therefore logical that a macroscopic property such as solubility is regulated primarily by the bromine atoms. Also, the various possibilities to position the C and S atoms in the Br “matrix” will seriously hamper a regular TBT order over a long range and so jeopardize the growth of a large (single) crystal as well as increase mosaic spread. Furthermore, the Br atoms effectively screen off the thiophene ring from the environment, such that the vibrational (and other) properties of a TBT molecule are little affected by the aggregation state it finds itself in.

Dipole Moment

As stated in the Introduction, the literature mentions measurements of the dipole moment of tetrabromothiophene by Keswani et al.¹ and by Shimozawa,² respectively. Keswani et al. use the Debye equation and calculate the dipole moment as being 0.73 D, using the experimental determined molar refraction R_D and the polarization at infinite dilution P_∞ . Shimozawa, however, publishes an experimental value of 0.12 D. The calculated dipole moments of tetrabromothiophene of the different geometries in Table 1 are listed in Table 3. Taking set V as the most

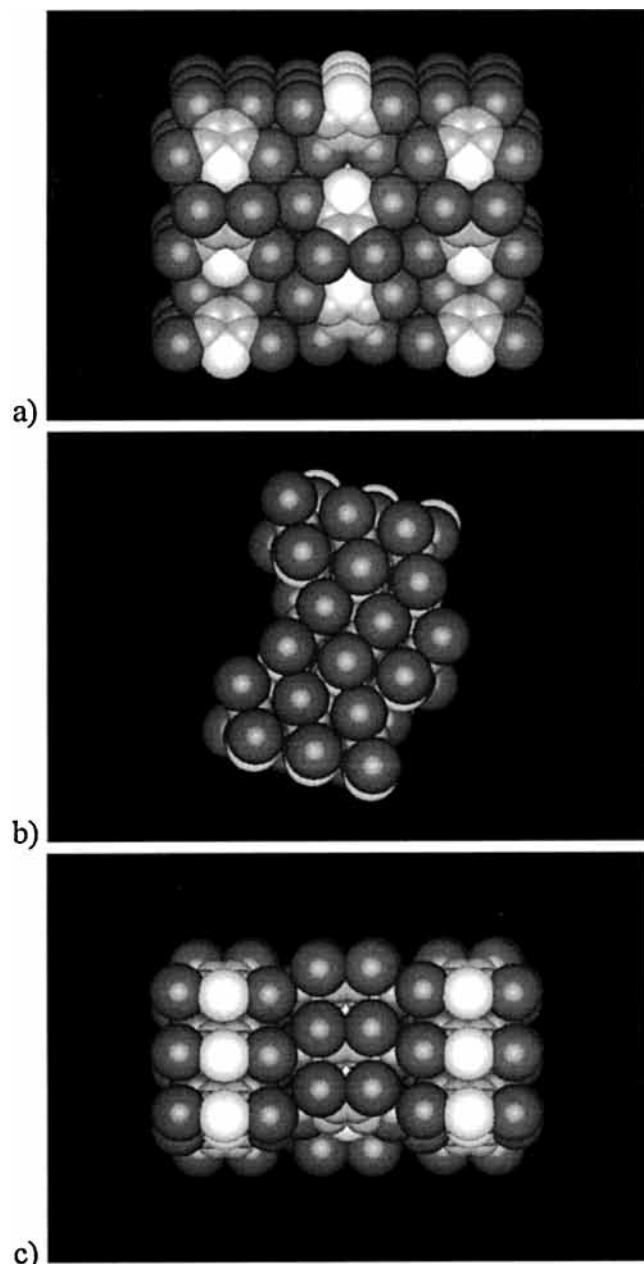


Figure 3. Plots of a section of the tetrabromothiophene crystal (27 molecules) displaying the crystal as a packing of bromine (brown) atoms interspersed with sulfur (yellow) and carbon (gray) atoms.

TABLE 3: Calculated Dipole Moments μ (D) of Tetrabromothiophene

	I	II	III	IV	V
	0.61	0.49	0.76	0.70	0.78

sophisticated, it is clearly seen that there is a good correspondence with Keswani's value; we must assume that Shimozawa's value suffers from a faulty experimental determination.

Conclusions

Hartree–Fock and density functional theoretical approaches at various levels of sophistication all agree that free tetrabromothiophene is a planar molecule with C_{2v} symmetry. The B3LYP/TZVP calculated force field was able, without additional scaling, to reproduce the Raman spectrum of TBT taken in the solid state with a root-mean-square deviation of 17 cm^{-1} and a

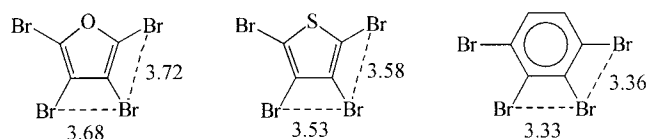


Figure 4. Structural formulas of TBT, tetrabromofurane (TBF), and 1,2,3,4-tetrabromobenzene (TBB) showing the influence of the ring type on Br...Br distances (Å). For TBF and TBB the calculations were performed at the HF/6-31G*(C,H,O)/6-311G*(Br) level in a planar conformation.

largest discrepancy of 39 cm^{-1} . This led (i) to a superior assignment of frequencies and (ii) to the observation of some line splittings due to crystal effects. These splittings allowed us to indicate $Pca2_1$ as the correct space group offered by powder X-ray diffraction experiments on TBT.¹¹ Nevertheless, the close match between the calculated “gas” phase vibrational frequencies and their experimental solid-state counterparts suggested that the molecule interacts only weakly with its environment in the crystal. This and some other solid-state properties could be rationalized from the packing observed in the crystalline state.¹¹ It is dominated by Br atoms striving for a close-packed Br arrangement frustrated by the structure of the molecule. The result is a dense Br matrix in which thiophene ring atoms are dispersed with restricted long range order.

This raises the question whether tetrabromothiophene is unique in this aspect. When the natural geometrical construction of the thiophene ring in TBT distorts the packing of the bromine atoms, similar compounds having other ring systems could more or less drastically change the bromine packing, and thus more or less drastically change the resulting chemical behavior. In view of this, it would be most interesting to compare the TBT results with those of tetrabromofurane, which has a more compact ring, and of 1,2,3,4-tetrabromobenzene, which has a more expanded ring (see Figure 4).

Acknowledgment. C.V.A. and W.H. thank the Flemish Science Foundation (FWO Vlaanderen) for an appointment as “onderzoeksdirecteur” and “post-doctoraal medewerker”, respectively. O.N.K. is grateful for postdoctoral grants given by “De Diensten van de Eerste Minister, DWTC” in 1997 and 1998. Financial support to the UA laboratories by the University of Antwerpen under grants GOA-BOF-UA, no. 23 and GOA-BOF-UA, no. 99/3/34, and by FWO Vlaanderen under grant G.0392.00 are gratefully acknowledged.

References and Notes

- (1) Keswani, R.; Freiser, H. *J. Am. Chem. Soc.* **1949**, *71*, 218.
- (2) Shimozawa, T. *Bull. Chem. Soc. Jpn.* **1965**, *38*, 1046.
- (3) Nordén, B. *Chem. Scr.* **1975**, *7*, 226.
- (4) Faniran, J. A. *Spectrochim. Acta* **1978**, *34A*, 379.
- (5) Sone, T.; Fujieda, K.; Takahashi, K. *Org. Magn. Reson.* **1975**, *7*, 572.
- (6) Dormidontov, Yu. P.; Grechishkin, V. S.; Gushchin, S. I. *Org. Magn. Reson.* **1972**, *4*, 599.
- (7) Degani, J.; Tundo, A.; Zauli, C. *Boll. Sci. Fac. Chim. Ind. Bologna* **1961**, *19*, 76.
- (8) Kohlrausch, K. W. F.; Schreiner, H. *Acta Phys. Austriaca* **1948**, *1*, 373.
- (9) Åkesson, B.; Gronowitz, S. *Ark. Kemi* **1967**, *28*, 155.
- (10) Bowie, J. H.; Cooks, R. G.; Lawesson, S. O.; Nolde, C. *J. Chem. Soc. B* **1967**, 616.
- (11) (a) Helmholdt, R. B.; Sonneveld, E. J.; Blockhuys, F.; Peeters, L. D.; Kataeva, O. N.; Lenstra, A. T. H.; Geise, H. J.; Schenk, H. Z. *Kristallogr.*, to be published. (b) Blockhuys, F. Ph.D. Thesis, University of Antwerpen (UIA), Belgium, Sept. 1999.
- (12) Paal, C. *Chem. Ber.* **1885**, 2253.
- (13) Steinkopf, W.; Jacob, H.; Penz, H. *Ann. Chem.* **1934**, *512*, 136.
- (14) Pulay, P. *Mol. Phys.* **1969**, *17*, 197.
- (15) Pulay, P. *Theor. Chim. Acta* **1979**, *50*, 299.

- (16) Van Alsenoy, C. *J. Comput. Chem.* **1988**, 9, 620.
- (17) Van Alsenoy, C.; Peeters, A. *J. Mol. Struct. (THEOCHEM)* **1993**, 286, 19.
- (18) Schäfer, L. *J. Mol. Struct.* **1983**, 100, 51.
- (19) Binkley, J. S.; Pople, J. A.; Hehre, W. J. *J. Am. Chem. Soc.* **1980**, 102, 939.
- (20) Gordon, M. S.; Binkley, J. S.; Pople, J. A.; Pietro, W. J.; Hehre, W. J. *J. Am. Chem. Soc.* **1982**, 104, 2797.
- (21) Pietro, W. J.; Francl, M. M.; Hehre, W. J.; DeFrees, D. J.; Pople, J. A.; Binkley, J. S. *J. Am. Chem. Soc.* **1982**, 104, 5039.
- (22) Dobbs, K. D.; Hehre, W. J. *J. Comput. Chem.* **1986**, 7, 359.
- (23) Hehre, W. J.; Ditchfield, R.; Pople, J. A. *J. Chem. Phys.* **1972**, 56, 2257.
- (24) Francl, M. M.; Pietro, W. J.; Hehre, W. J.; Binkley, J. S.; Gordon, M. S.; DeFrees, D. J.; Pople, J. A. *J. Chem. Phys.* **1982**, 77, 3654.
- (25) Curtiss, L. A.; McGrath, M. P.; Blandeau, J. P.; Davis, N. E.; Binning, R. C.; Radom, L. *J. Chem. Phys.* **1995**, 103, 6104.
- (26) Schäfer, A.; Horn, H.; Ahlrichs, R. *J. Chem. Phys.* **1992**, 97, 2571.
- (27) Becke, A. D. *J. Chem. Phys.* **1994**, 98, 5648.
- (28) Schäfer, A.; Huber, C.; Ahlrichs, R. *J. Chem. Phys.* **1994**, 100, 5829.
- (29) M. J. Frisch, G. W. Trucks, H. B. Schlegel, P. M. W. Gill, B. G. Johnson, M. A. Robb, J. R. Cheeseman, T. Keith, G. A. Petersson, J. A. Montgomery, K. Raghavachari, M. A. Al-Laham, V. G. Zakrzewski, J. V. Ortiz, J. B. Foresman, J. Cioslowski, B. B. Stefanov, A. Nanayakkara, M. Challacombe, C. Y. Peng, P. Y. Ayala, W. Chen, M. W. Wong, J. L. Andres, E. S. Replogle, R. Gomperts, R. L. Martin, D. J. Fox, J. S. Binkely, D. J. Defrees, J. Baker, J. P. Stewart, M. Head-Gordon, C. Gonzalez, J. A. Pople. *Gaussian 94*, Revision D.4; Gaussian, Inc.: Pittsburgh, PA, 1995.